EUROPEAN ORGANIZATION FOR NUCLEAR RESEARCH

Letter of Intent to the ISOLDE and Neutron Time-of-Flight Committee

Production of ^{169}Yb for calibration of a transition-edge sensor for precision x-ray spectroscopy of antiprotonic atoms

October 2, 2024

Hiroyuki Fujioka[1], Takashi Higuchi[2], Ben Ohayon[3], Nancy Paul[4], Michael Roosa[4], Juliana Schell[5,6]

[1] *Department of Physics, Institute of Science Tokyo, Meguro, Tokyo 152-8551, Japan*
[2] *Institute for Integrated Radiation and Nuclear Science, Kyoto University, Osaka 590-0494, Japan*
[3] *The Helen Diller Quantum Center, Department of Physics, Technion - Israel Institute of Technology, Haifa 3200003, Israel*
[4] *Laboratoire Kastler Brossel, 4, place Jussieu, 75005 Paris, France*
[5] *CERN, Esplanade des Particules 1, 1211 Geneva, Switzerland*
[6] *Institute for Materials Science and Center for Nanointegration Duisburg-Essen (CENIDE), University of Duisburg-Essen, 45141 Essen, Germany*

Spokespersons: Takashi Higuchi [higuchi.takashi.8k@kyoto-u.ac.jp], Nancy Paul [nancy.paul@lkb.upmc.fr]
Contact person: Juliana Schell [juliana.schell@cern.ch]

Abstract: The PAX (antiProtonic Atom X-ray spectroscopy) project introduces a novel approach to stringently test bound-state quantum electrodynamics (BSQED) through high-precision x-ray spectroscopy of Rydberg antiprotonic atoms. Measurements of x rays in a 30–200 keV range with eV-level precision are made possible by the emerging multipixel transition-edge sensor (TES) superconducting microcalorimeter technology. The key for the experiment in a harsh background environment is calibration of a TES detector using well-known γ rays. We have identified ^{169}Yb as an ideal calibration source for a TES detector in a 100–200 keV energy range and propose its production and collection at ISOLDE for upcoming PAX test beam experiments at the Antiproton Decelerator.

CERN-INTC-2024-052 / INTC-I-280
02/10/2024

Summary of requested shifts: 4 shifts, (split into 2 runs over 1 or 2 years)

1 Introduction

PAX (antiProtonic Atom X-ray spectroscopy) The fundamental motivation of this project is to perform stringent tests of strong field quantum electrodynamics (QED) by high-precision x-ray spectroscopy of Rydberg transitions in antiprotonic atoms. QED is the best understood quantum field theory, serving as the foundation for searches for physics Beyond the Standard Model with atoms at the precision frontier. Bound-state QED (BSQED) allows extremely precise calculations for few-electron systems. However, in the strong field regime where the effect of αZ can no longer be treated perturbatively, the theory is poorly tested. For the case of precision spectroscopy of highly-charged ion (HCI) systems, which provides some of the best tests of strong-field BSQED, the theory has only barely been probed beyond the first order [1]. The fundamental limitations of HCI systems arise from limited knowledge of nuclear properties, such as the finite nuclear size (NFS), nuclear polarization, and/or deformation. These factors significantly contribute to the transition energies influenced by strong fields, thereby hindering precise comparisons between theoretical calculations and experimental results. As an example, contributions of the NFS effect to the theoretical uncertainties of HCI Lyman-α transition energies are shown in Figure 1 in comparison to the QED contributions and the experimental uncertainties.

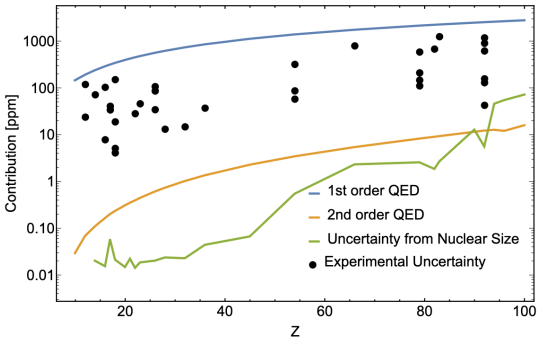

Figure 1: The QED contributions to the Lyman-α transition energy of a HCI, scaled by Z^4 as a function of Z, compared with experimental uncertainty and uncertainty on the theoretical energy due to uncertainties in the nuclear size. Figure from Ref. [2].

In this context, the PAX (antiProtonic Atom X-ray spectroscopy) project introduces a novel approach for testing strong-field BSQED using antiprotonic atoms, where an antiproton replaces the electron in atomic orbitals [2]. Upon formation, the antiproton is captured in an excited state and subsequently cascades down, emitting characteristic x rays. Because the Bohr radius of an antiprotonic atom is smaller than that of an ordinary atom by the antiproton-to-electron mass ratio ($\approx$1836), the antiproton experiences Coulomb fields that are orders of magnitude stronger than those experienced by its electronic counterpart. To suppress the nuclear effects, a series of transitions between circular $(n, l = n-1)$ Rydberg states have been identified, where the atomic orbitals have little to no overlap with the nucleus [2]. Some of the proposed transitions are given in Table 1, compared to the Lyman-α transition of hydrogen-like ^{238}U, which provides one of the current best tests of strong-field BSQED. For this transition, with an energy of $\approx$ 100 keV, the first and second-order QED contribute 0.25% and 0.0012%, respectively, while nuclear effects account for 0.19%. The experimental uncertainty of 4.3 eV primarily tests first-order QED, with the precision limited by nuclear uncertainty. In contrast, the $12o_{23/2} \rightarrow 11n_{21/2}$ transition of the antiprotonic ^{132}Xe ($\bar{p}^{132}$Xe) atom benefits from threefold-enhanced QED effects, with the nuclear effects reduced by a factor of 100.

Transition-Edge Sensor The target antiprotonic atom transition energies of PAX lie within a range of 30–200 keV. The key for the experimental realization of these high precision x-ray measurements are multipixel transition-edge sensor (TES) superconducting microcalorimeters, which provide high resolution (10^{-4} intrinsic resolution) and high detection efficiency (0.4 quantum efficiency) [4]. Although even higher energy resolution can be achieved by conventional

Table 1: Part of transitions of antiprotonic atoms proposed for strong-field BSQED tests by PAX from Ref. [2]. The Lyman-α transition of hydrogen-like ^{238}U is included for comparison, whose experimental value is based on Ref. [3]. All energies in eV.

Particle	Element	States	Theoretical Trans. energy	1st order QED	2nd order QED	FNS	Experiment
e^-	^{238}U	$2p_{3/2} \to 1s_{1/2}$	102175.0991	−257.2281	1.2278	−198.5110	102178.1(4.3)
$\bar{p}$	^{10}Ar	$6h_{11/2} \to 5g_{9/2}$	97106.9649	524.4499	5.1711	1.0708	
$\bar{p}$	^{84}Kr	$9l_{17/2} \to 8k_{15/2}$	105534.2121	505.733	4.8592	1.0625	
$\bar{p}$	^{132}Xe	$12o_{23/2} \to 11n_{21/2}$	95937.8536	398.8736	3.7548	0.7860	

crystal spectrometers, it comes with a cost of severely reduced detection efficiency and limited energy range. Having both high resolution and high detection efficiency, a TES opens up the possibility of precision x-ray spectroscopy of exotic atoms where luminosity is limited. For the PAX TES, the expected intrinsic energy resolution in the energy range of interest is expected to be ≈ 50 eV, which is an order of magnitude better than conventional germanium (Ge) detectors. Due to its operational principle, a TES is a highly non-linear detector system. As such, it is necessary to have known calibration lines within a few percent of the transition energy both above and below each new line being studied. This is a method developed within the PAX team and collaborators performing x-ray spectroscopy on muonic atoms within the HEATES and QUARTET collaborations at J-PARC and PSI, respectively[5, 6]. The most recent result from the HEATES measurement with a TES successfully achieved calibration accuracies at the level of 10^{-5} [5]. The next step is to demonstrate the TES operation with an antiproton beam from the Extra Low Energy Antiproton (ELENA) ring at the Antiproton Decelerator (AD).

Test beam proposal at the AD/TELMAX To address these issues and demonstrate the feasibility of the PAX project, we have submitted a test beam proposal to AD/ELENA for 2025. The test beam experiment will be conducted at TELMAX, a test beam area newly made available in the AD. The objectives of the test beam experiment are (i) to test a prototype TES detector with ELENA and study the background in this environment, (ii) to test antiproton extraction schemes from ELENA and study their influences on the detector, and (iii) to study the accuracy and stability of the energy calibration required for eV precision under these conditions.
A set of targets for the test beam experiment is provided in Table 2. The antiprotonic transitions of these atoms cover the entire detection range of the TES detector from 30–300 keV, and have been studied in previous experiments at CERN/LEAR and BNL-AGS [7, 8], which enables to benchmark the obtained data with the literature. Figure 2 shows simulated spectra for the antiprotonic ^{40}Ca ($\bar{p}^{40}$Ca) transition, highlighting the improved resolution of the TES detector (50 eV FWHM) compared to the previous x-ray spectroscopy with a high-purity Ge (HPGe) detector (700 eV FWHM).

2 Calibration of a TES detector with ^{169}Yb

TES calibration at $<$ 10 keV demonstrated at J-PARC As mentioned earlier, calibration of the TES detector is crucial for exotic atom spectroscopy in accelerator facilities. In the recent J-PARC experiment, which characterized the $n = 5 \to 4$ transitions of the muonic Ne (μNe) atom, energy deposits by charged particles were found to heat the TES pixel frame and to cause significant shifts in its energy calibration [5].

Table 2: Energies of antiprotonic X-rays for targets selected for the 2025 PAX test beam experiment at AD/TELMAX with ELENA antiproton beams. All targets are with natural isotopic abundance.

Element	Transition	Energy (keV)
$^{28-30}$Si	$6h \to 5g$	58
$^{28-30}$Si	$5g \to 4f$	107
^{40,44}Ca	$6h \to 5g$	119
$^{90-96}$Zr	$8j \to 7i$	190

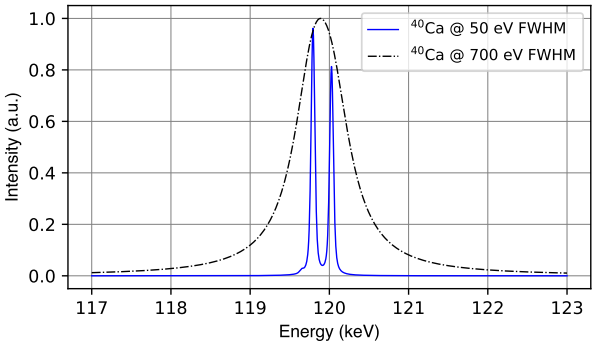

Figure 2: Simulated spectra of the $\bar{p}^{40}$Ca transition. The black dashed line represents a spectrum with a resolution of a HPGe detector of PS209 at LEAR [8]. The blue solid line represents the one expected by a 50-eV resolution TES, where the fine sturcture is resolved.

To track and correct for these shifts, calibration x rays near the target transition energy were generated by x-ray tubes and continuously monitored during the measurements. Through time-dependent studies based on measurements of these calibration lines, a systematic uncertainty of 0.13 eV out of the 6297.080 eV transition energy was obtained, dominated by correction uncertainties of thermal crosstalk between the TES pixels [5]. For comparison, the calibration uncertainty was a factor of two smaller.

^{169}Yb as a calibration source The challenge for TES calibration in the energy range proposed for PAX lies particularly between 100 keV and 200 keV, where x-ray tubes are unavailable and impractical due to the large natural linewidth of the K-α transitions, and a relatively scarce number of γ sources exist with well-known lines. A list of nuclides with γ-ray energies known to better than 10 p.p.m. has been compiled by Helmer and van der Leun as recommended standards for detector calibration[1] [9]. An excerpt relevant to PAX is shown in Table 3, where it is clear that ^{169}Yb is an excellent calibration source in this energy range. In fact, along with ^{182}Ta, ^{169}Yb is one of the nuclides whose γ-ray energies have been measured with the highest precision using a double-crystal spectrometer [10]. Used together with commercially available sources such as ^{57}Co and ^{152}Eu, it will enable systematic studies of TES calibration. The emission intensities of these ^{169}Yb calibration lines are between 1.874% and 43.62% (see Table 4).

Strategy for 100–200 keV TES calibration with ^{169}Yb In Figure 3(b), the effectiveness of ^{169}Yb as a calibration source is demonstrated by taking the $\bar{p}^{40}$Ca atom transition ($\approx$ 120 keV) as an example. If only commercially available sources of ^{57}Co and ^{152}Eu are used, three lines (122, 123, and 136 keV) above the target transition are available. Adding ^{169}Yb would provide four more lines within $\pm$30 keV of the target transition, both on the lower and higher energy sides. This would enable the application of systematic studies developed for the muonic atom experiment, such as (i) assessing the robustness of calibration by comparing calibration functions based on different combinations of lines, and (ii) constructing calibration functions using higher-order polynomials or spline, and comparing them to estimate calibration uncertainty (see Figure 3(a)).

Production and collection of ^{169}Yb at ISOLDE In this letter, we propose production of ^{169}Yb for calibration of the TES detector in 100–200 keV energies. Although ^{169}Yb is not com-

[1]Note that nuclides with half lives over 30 days practical for the use are listed in the table as the parent nuclides. The γ-rays are not necessarily from the direct decay of the parent nuclides. For example, the γ-rays of ^{172}Hf–^{172}Lu in the table are from the intemediate ^{172m}Lu.

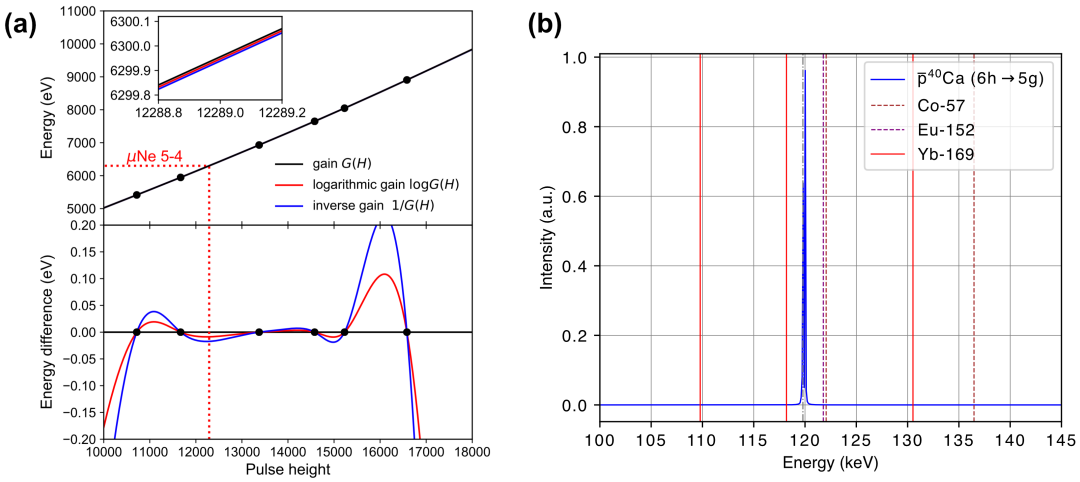

Figure 3: (a) TES calibration at J-PARC. Around the μNe $n = 5 \rightarrow 4$ line at ≈ 6.3 keV, the six data points (black dots) were obtained using Cr, Co, and Cu x-ray tubes. The red and blue calibration curves were constructed by spline functions assuming different gain dependencies. The inset shows the pulse height-to-energy conversion with the two calibration functions, resulting in calibration ambiguity of 0.01 eV. Reproduced from Ref. [5]. (b) Calibration lines provided by ^{169}Yb around 120 keV, shown with the spectrum of the $\bar{p}^{40}$Ca transition (Figure 2). The lines from commercially available sources and those from ^{169}Yb are indicated by the dashed and the solid lines, respectively.

mercially available in a form compatible for detector calibration, production within a reasonable time is possible at ISOLDE. The produced ^{169}Yb is planned to be used for the PAX test beam time at AD/TELMAX, currently being requested for April or May 2025.

In order to expose all the 100 pixels of the PAX prototype TES, we require about 100 cps on the detector array. Assuming 10^{-2} of a geometrical factor from the solid angle, and further attenuation by 10^{-2} through the stainless steel vacuum flange, we set our goal activation to be 1 MBq at the time of the AD beamtime.

The ^{169}Yb yield at ISOLDE upon collection is 1.90×10^8 μC^{-1} [11]. In Fig. 4(a), the ^{169}Yb activity right after collection is shown as a function of time, assuming nominal proton beam currents from 0.5 to 2.0 μA (corresponding to 1.52×10^8–3.80×10^8 particles per second (pps)). Because of the rather short half life of ^{169}Yb (30.026 d), the production at ISOLDE is preferably arranged in a timely manner to be shortly before the AD beamtime. In Fig. 4(b), the activity at the time of the AD experiment is shown as a function of ISOLDE collection time in hours and days between the ISOLDE and the AD beamtimes. For example, if the interval between the two experiments is within 30 days, 12 hours of collection is sufficient.

The feasibility of this collection experiment has been thoroughly evaluated from several aspects. The collection substrate will be either an aluminum or a polymer film, in which a 30 keV Yb$^+$ beam will be stopped in a range of about 50 nm, making the γ attenuation negligible.

Potential contaminant nuclides that would be collected with ^{169}Yb have also been carefully evaluated and confirmed not to cause any serious issue (see section 3.2).

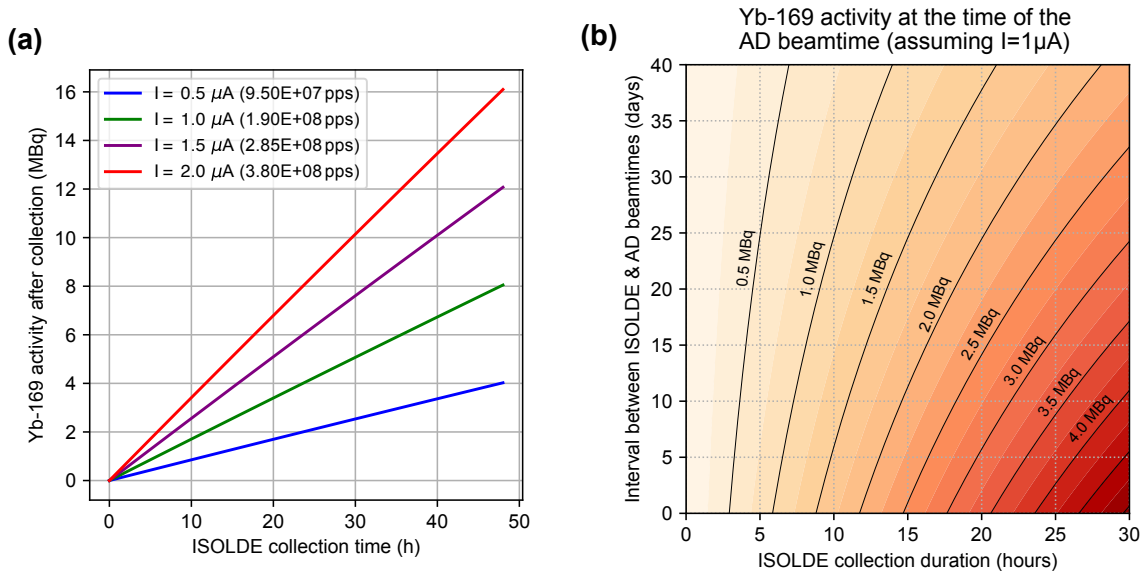

Figure 4: (a) ^{169}Yb activity after collection at ISOLDE, assuming different proton beam currents from 0.5 to 2 μA. (b) ^{169}Yb activity at the AD experiment as a function of ISOLDE collection time and time between ISOLDE and AD beamtimes, assuming a proton beam current of 1 μA.

Table 3: A list of recommended γ-ray sources for detector calibration from Ref. [9], excerpted for an energy range relevant for the PAX project. Commercial sources in preparation are marked with *. Seven transitions of ^{169}Yb are marked with †.

E_γ(keV)	Parent nuclide
40.583 23 (17)	^{99}Mo
48.915 33 (5)	^{161}Tb
53.162 2 (6)*	^{133}Ba
57.191 7 (3)	^{161}Tb
59.540 9 (1)*	^{241}Am
63.120 44 (4)†	^{169}Yb
65.722 15 (15)	^{182}Ta
66.051 8 (8)	^{75}Se
67.749 70 (10)	^{182}Ta
69.673 00 (13)	^{153}Sm, ^{153}Gd
74.566 69 (6)	^{161}Tb
78.742 2 (6)	^{172}Hf–^{172}Lu
81.750 9 (5)	^{172}Hf–^{172}Lu
84.254 74 (8)	^{170}Tm
84.680 24 (26)	^{182}Ta
86.787 7 (3)	^{160}Tb
93.614 47 (8)†	^{169}Yb
96.734 0 (9)	^{75}Se
97.431 00 (21)	^{153}Sm, ^{153}Gd
100.105 95 (7)	^{182}Ta
103.180 12 (17)	^{153}Sm, ^{153}Gd
109.779 24 (4)†	^{169}Yb

E_γ(keV)	Parent nuclide
113.671 70 (22)	^{182}Ta
116.417 9 (6)	^{182}Ta
118.189 40 (14)†	^{169}Yb
121.115 5 (11)	^{75}Se
121.7817(3)*	^{152}Eu
122.060 65 (12)*	^{57}Co
123.070 6 (9)	^{154}Eu
130.522 93 (6)†	^{169}Yb
136.000 1 (6)	^{75}Sb
136.473 56 (29)*	^{57}Co
140.511 (1)	^{99}Mo
145.443 3 (14)	^{141}Ce
152.429 91 (26)	^{182}Ta
156.386 4 (3)	^{182}Ta
160.612 0 (16)*	^{133}Ba
165.857 5 (11)	^{139}Ce
172.853 07 (21)	^{153}Sm, ^{153}Gd
176.314 (2)	^{125}Sb
177.213 07 (6)†	^{169}Yb
179.393 81 (25)	^{182}Ta
197.034 1 (10)	^{160}Tb
197.956 75 (7)†	^{169}Yb

References

[1] R. Loetzsch et al., Nature **625**, 673–678 (2024).

[2] N. Paul et al., Phys. Rev. Lett. **126**, 173001 (2021).

[3] A. Gumberidze et al., Phys. Rev. Lett. **94**, 223001 (2005).

[4] J.N. Ullom and D.A. Bennett, Rev. Sci. Inst. **28**, 084003 (2015)

[5] T. Okumura et al. Phys. Rev. Lett. **130** (2023) 173001.

[6] B. Ohayon et al., Physics 2024,

[7] P. Roberson et al., Phys. Rev. C **16**, 1945(1977)

[8] F.J. Hartmann et al. Phys. Rev. C **65**, 014306 (2001).

[9] R.G. Helmer and C. van der Leun, Nucl. Inst. Meth. A **450**, 35 (2000).

[10] E.G. Kessler Jr. et al., Nucl. Inst. Meth. **160**, 435 (1979).

[11] ISOLDE Yield Database: `https://isoyields2.web.cern.ch/Yield_Home.aspx`

[12] IAEA Nuclear Data Services: `https://www-nds.iaea.org/`

[13] V. Fedosseev et al., J. Phys. G. **44**, 084006 (2017).

[14] G.J. Beyer et al., Nucl. Inst. Meth. **146**, 419 (1977).

[15] M.J.G Borge, EPJ Web Conf. **117**, 10002 (2016)

3 Details for the Technical Advisory Committee

3.1 General information

Describe the setup which will be used for the measurement. If necessary, copy the list for each setup used.

☒ Permanent ISOLDE setup: SSP implantation chamber

- ☒ To be used without any modification
- ☐ To be modified: *Short description of required modifications.*

☐ Travelling setup (*Contact the ISOLDE physics coordinator with details.*)

- ☐ Existing setup, used previously at ISOLDE: *Specify name and IS-number(s)*
- ☐ Existing setup, not yet used at ISOLDE: *Short description*
- ☐ New setup: *Short description*

3.2 Beam production

For any inquiries related to this matter, reach out to the target team and/or RILIS (please do not wait until the last minute!). For Letters of Intent focusing on element (or isotope) specific beam development, this section can be filled in more loosely.

- Requested beams:

Isotope	Production yield in focal point of the separator ($/\mu$C)	Minimum required rate at experiment (pps)	$t_{1/2}$
Isotope 1:^{169}Yb Isotope 2 Isotope 3	1.90×10^8	9.5×10^7*	32.018 d

*** The collection can still be performed with a lower rate. However, the collection time needs to be extended to have the same total collection (see Figure 4).**

- Full reference of yield information: ISOLDE yield database [11], confirmed by Sebastian Rothe.
- Target - ion source combination: Target: Ta foil, ion source: RILIS (^{169}Yb$^+$)
- RILIS?: Yes
  - ☐ Special requirements: (*isomer selectivity, LIST, PI-LIST, laser scanning, laser shutter access, etc.*)
- Additional features?
  - ☐ Neutron converter: (*for isotopes 1, 2 but not for isotope 3.*)
  - ☐ Other: (*quartz transfer line, gas leak for molecular beams, prototype target, etc.*)
- Expected contaminants:

  Since our purpose is to produce a γ-ray source, only unstable contaminants are of potential issues. The dominant contaminants are expected in the isobar of ^{169}Yb, but to be conservative, we estimated potential yields of contaminants within the mass numbers

$A = 168$–170. Among them, those with half lives longer than 1 day are marked in Figure 5 and listed in Table 4. Among them, ^{169}Lu decays into ^{169}Yb, so it would not be a problem. The γ-ray energies of ^{169}Er and ^{170}Tm are well known, so they would not be an issue, either. What could be of potential issue are ^{168}Tm and ^{170}Lu, which emit γ-rays that are not known with high precision.

Except ^{169}Yb, only the in-target yield is available from the yield database. Therefore, in order to estimate the collection yields for the contaminants, we assume the following relation between the in-target yield Y_{target} and the collection yield Y_{collect}

$$Y_{\text{collect}} = \epsilon_{\text{sep}}\epsilon_{\text{ext}}\epsilon_{\text{ion}}Y_{\text{target}}, \tag{1}$$

where $\epsilon_{\text{sep}}\epsilon_{\text{ext}}$ and ϵ_{ion} account for, the transmission efficiency through the separator, the extraction efficiency from the production target, and the ionization efficiency, respectively. To obtain an estimate of the relative efficiency against^{169}Yb, we further assume for a nuclide (Z, A),

$$\epsilon_{\text{ion}}^{(Z\neq 70,A)} = \epsilon_{\text{ion}}^{(Z=70,A)}/20 \tag{2}$$

$$\epsilon_{\text{ext}}^{(Z\neq 70,A)} = \epsilon_{\text{ext}}^{(Z=70,A)} \tag{3}$$

$$\epsilon_{\text{sep}}^{(Z,A\neq 169)} = \epsilon_{\text{sep}}^{(Z,A=169)}/10. \tag{4}$$

The factor of 20 between the laser ionization for Yb and the surface ionization for off-resonant ions (Eq. (2)) is from Ref. [13]. Regarding Eq. (3), the ϵ_{ext} of the neighboring contaminant ions are on the same order as Yb according to Ref.[14]. More realistically, it should be further suppressed for Lu and Er which have higher boiling points than 2000 ℃. As for Eq. (4), although the separator resolution of GPS is specified to be ≈ 1000 [15], we assume 1/10 of separator transmission for the contaminants with $\Delta A = \pm 1$ as compared to ^{169}Yb, to be very conservative.

For each contaminant nuclide, the conservatively estimated collection yield and the activities at the end of collection, and after 20 days of decay are listed in Table 4. Here, we can see that the activities of the contaminants are at least three orders of magnitudes lower than ^{169}Yb. Although we can conclude that this collection experiment is robust against contaminants, understanding the activties of each contaminant and identifying its γ-ray energies could give significant advantages for the low S/N experiment in the AD. Therefore, we would like to conduct an explicit characterization of the contaminants by the yield measurement during the beam tuning, or with an HPGe measurement after the collection.

Isotopes and yields

- Acceptable level of contaminants: $< 5 \times 10^{-3}$, which is assumed in the estimates above.
- Can the experiment accept molecular beams?: Yes, unless there is loss in the yield
- Are there any potential synergies (same element/isotope) with other proposals and LOIs that you are aware of?: Not that we are aware of.

3.3 HIE-ISOLDE

Not applicable. We will not use the HIE-ISOLDE.

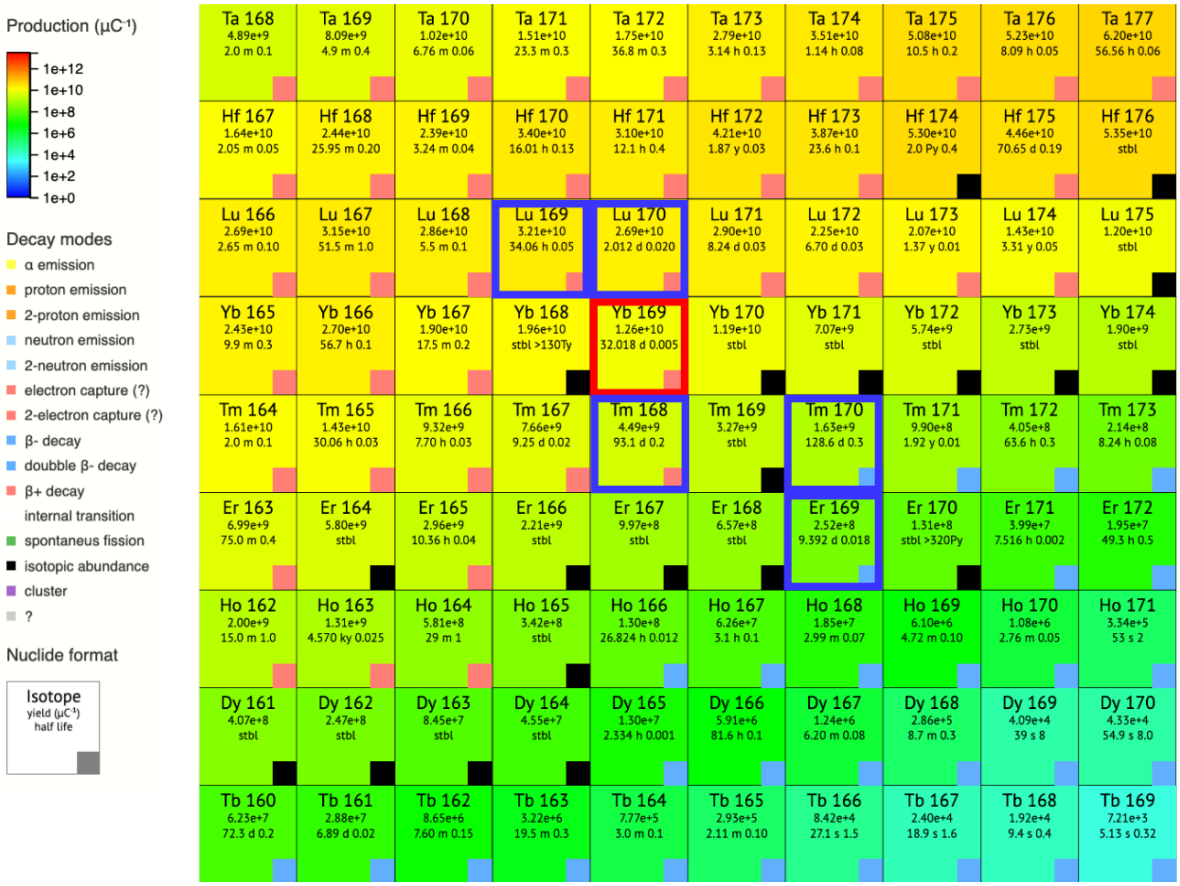

Figure 5: The in-target production yield from the ISOLDE yield database for the Ta foil target with a beam energy of 1.4 GeV, based on ABRABLA [11]. ^{169}Yb is marked in red. The unstable nuclides of half lives longer than 1 day and the mass numbers within $A = 168$–170 are marked in blue.

Table 4: Decay modes and γ-ray emissions are listed for the potential contaminant nuclides. Data from Ref. [12]. Branching ratios or emission intensities smaller than 5×10^{-3} are ignored.

A	Nuclide	$T_{1/2}$	Decay modes (B.R.)	E_γ (keV)	I_γ (%)
169	^{169}Yb	32.018(5) d	E.C.$\rightarrow^{169}$Tm (100%)	50.61	< 0.5390
				50.86	< 0.5390
				63.01	< 2.156
				63.12044 (3)	43.62 (23)
				93.61447 (7)	2.580 (17)
				109.77924 (3)	17.39 (9)
				118.18940 (14)	1.874 (10)
				129.94	< 0.5390
				130.52293 (4)	11.38 (5)
				177.21307 (4)	22.28 (11)
				$\geq$ 197.95675 (4)	$\leq$ 35.95 (12)
169	^{169}Lu	34.06(5) h	E.C., $\beta^+ \rightarrow^{169}$Yb (100%)	(same above)	(same above)
169	^{169}Er	9.392(18) d	$\beta^- \rightarrow^{169}$Tm (100%)	8.4107 (15)	0.170 (19)
168	^{168}Tm	93.1(2) d	E.C., $\beta^+ \rightarrow^{168}$Er (99.990 (7)%)	79.804 (2)	10.95 (22)
			$\beta^- \rightarrow^{168}$Yb (0.010 (7)%)	99.289 (2)	4.234 (22)
				184.295 (2)	18.15 (16)
				$\geq$ 198.251 (2)	$\leq$ 54.49 (16)
170	^{170}Lu	2.012 (30) d	E.C., $\beta^+ \rightarrow^{170}$Yb (100%)	84.262 (4)	8.7 (6)
				152.60 (3)	0.273 (14)
				$\geq$ 193.13 (5)	$\leq$ 5.9 (3)
170	^{170}Tm	128.6 (3) d	$\beta^- \rightarrow^{170}$Yb (99.869 (10)%)	84.25474 (8)	2.48 (6)
			E.C.$\rightarrow^{170}$Er (0.131 (10)%)		

Table 5: Expected yields, and the expected activities at the end of the collection and after decay of 20 days, are listed for ^{169}Yb and the contaminant nuclides. Conservative estimates are made for contaminant nuclides based on Eqs. (1–4).

Nuclide	In-target yield (μC^{-1})	Collection yield (μC^{-1})	Activity after 12-h collection	Activity after 20-day decay
^{169}Yb	1.26×10^{10}	1.90×10^{8}	2.05 MBq	1.33 MBq
^{169}Lu	3.21×10^{10}	$\leq 2.47 \times 10^{7}$	$\leq$ 5.24 MBq	$\leq$ 300 Bq
^{169}Er	2.52×10^{8}	$\leq 1.90 \times 10^{5}$	$\leq$ 6.88 kBq	$\leq$ 1.57 kBq
^{168}Tm	4.49×10^{9}	$\leq 3.39 \times 10^{5}$	$\leq$ 1.26 kBq	$\leq$ 1.08 kBq
^{170}Lu	2.69×10^{10}	$\leq 2.03 \times 10^{6}$	$\leq$ 321 kBq	$\leq$ 327 Bq
^{170}Tm	1.63×10^{9}	$\leq 1.23 \times 10^{5}$	$\leq$ 331 Bq	$\leq$ 297 Bq

For any inquiries related to this matter, reach out to the ISOLDE machine supervisors (please do not wait until the last minute!).

- HIE ISOLDE Energy: *(MeV/u); (exact energy or acceptable energy range)*
  - ☐ Precise energy determination required
  - ☐ Requires stable beam from REX-EBIS for calibration/setup? *Isotope?*
- REX-EBIS timing
  - ☐ Slow extraction
  - ☐ Other timing requests
- Which beam diagnostics are available in the setup?
- What is the vacuum level achievable in your setup?

3.4 Shift breakdown

Summary of requested shifts:
N.B.: Here, a scenario of having about 30 days of interval between the ISOLDE and AD beamtimes, and a nominal proton beam current of 1 μA is assumed. In that case, 12 hours (1.5 shifts) should be sufficient for collection of the required activity of ^{169}Yb. (see Figure 4)

We would like to request two runs, each consisting of two shifts with proton beams, in a period of 2025–2026 before the AD beamtimes for PAX. For 2025, the PAX test beam is currently being requested for April–May 2025.

Without protons	Requested shifts
Stable beam from separator (before run)	0.25
RILIS and beamline tuning	0.25
With protons	Requested shifts
Collection	2.0

Subtotal per run: without protons: 0.5 shifts, With protons: 2 shifts
Total of 2 runs: without protons: 1.0 shifts, With protons: 4 shifts

3.5 Health, Safety and Environmental aspects

3.5.1 Radiation Protection

- If radioactive sources are required: not applicable.
  - Purpose?
  - Isotopic composition?
  - Activity?
  - Sealed/unsealed?
- For collections:
  - Number of samples?: One
  - Activity/atoms implanted per sample?: 2 MBq (collected on the surface of either aluminum or polypropylene substrate)
  - Post-collection activities?: Shipping to the AD (will be arranged with the CERN shipping service. A container to reduce the surface radiation dose will be prepared if required)

N.B.: Here again, 12-h collection with a 1 μA proton beam is the basis of this estimate, assuming about 30 days of interval between the ISOLDE and AD experiments. The goal activity may differ depending on the ISOLDE-AD interval.

3.5.2 Only for traveling setups

Not applicable. We will use the permanent setup.

- Design and manufacturing
  - ☒ Consists of standard equipment supplied by a manufacturer
  - ☐ CERN/collaboration responsible for the design and/or manufacturing
- Describe the hazards generated by the experiment:

Domain	Hazards/Hazardous Activities		Description
Mechanical Safety	Pressure	☐	[pressure] [bar], [volume][l]
	Vacuum	☐	
	Machine tools	☐	
	Mechanical energy (moving parts)	☐	
	Hot/Cold surfaces	☐	
Cryogenic Safety	Cryogenic fluid	☐	[fluid] [m3]
Electrical Safety	Electrical equipment and installations	☐	[voltage] [V], [current] [A]
	High Voltage equipment	☐	[voltage] [V]
Chemical Safety	CMR (carcinogens, mutagens and toxic to reproduction)	☐	[fluid], [quantity]
	Toxic/Irritant	☐	[fluid], [quantity]
	Corrosive	☐	[fluid], [quantity]
	Oxidizing	☐	[fluid], [quantity]
	Flammable/Potentially explosive atmospheres	☐	[fluid], [quantity]

	Dangerous for the environment	☐	[fluid], [quantity]
Non-ionizing radiation Safety	Laser	☐	[laser], [class]
	UV light	☐	
	Magnetic field	☐	[magnetic field] [T]
Workplace	Excessive noise	☐	
	Working outside normal working hours	☐	
	Working at height (climbing platforms, etc.)	☐	
	Outdoor activities	☐	
Fire Safety	Ignition sources	☐	
	Combustible Materials	☐	
	Hot Work (e.g. welding, grinding)	☐	
Other hazards			